UCRL-

UNCLASSIFIED

UNIVERSITY OF CALIFORNIA — BERKELEY

RADIATION LABORATORY

DISCLAIMER

UCRL-1495
Unclassified-Physics-Distribution

UNIVERSITY OF CALIFORNIA

Radiation Laboratory

Contract No. W-7405-eng-48

FURTHER RESULTS ON THE PRODUCTION OF NEUTRAL MESONS BY PHOTONS

Wolfgang K. H. Panofsky, Jack Steinberger, and Jack Steller

October 1, 1951

Berkeley, California

FURTHER RESULTS ON THE PRODUCTION OF NEUTRAL MESONS BY PHOTONS

Wolfgang K. H. Panofsky,* Jack Steinberger,** Jack Steller

Radiation Laboratory, Department of Physics,
University of California, Berkeley, California

October 1, 1951

Abstract

Further measurements have been made on the photoproduction of neutral mesons using the gamma-gamma coincidence technique. New data have been obtained on the gamma-gamma correlation curves in beryllium. The angular distribution of the photo mesons in Be has been determined and found to be strongly peaked forward. The dependence on the atomic number A of production has been found to obey an $A^{2/3}$ law. Some data obtained for production in hydrogen show that the π^0 and π^+ production cross sections are comparable and that the π^0 excitation curve starts more slowly from threshold than does the π^+ photo excitation curve.

*Now at Stanford University.
**Now at Columbia University.

FURTHER RESULTS ON THE PRODUCTION OF NEUTRAL MESONS BY PHOTONS

Wolfgang K. H. Panofsky,* Jack Steinberger,** Jack Steller

Radiation Laboratory, Department of Physics,
University of California, Berkeley, California

October 1, 1951

A. Introduction

In a previous paper[1] we have discussed the evidence for photoproduction of neutral mesons. Since the time of our last report considerable progress has been made concerning our information on this particle. The charge exchange reaction[2] has given evidence as to the mass of the π^0 meson. A. Sachs and J. Steinberger[3] have shown that the π^0 formed by π^- capture in hydrogen gives gamma-gamma coincidences as has been established for photo produced π^0's. Also, further data on the production of π^0 mesons from proton collisions are available.[4] Cosmic ray evidence[5] in photographic plates has shown that $\pi^\pm$ and π^0 mesons are produced by primaries in comparable numbers if one infers that single electron-positron pairs correlated to high energy stars are evidence of π^0 mesons. Thus there is now evidence as to the existence of a π^0 meson and also as to its spin and intrinsic parity.

B. Instrumentation

This paper deals with further results on the photoproduction in the 325 Mev x-ray beam of the Berkeley synchrotron. The geometrical disposition of internal target, x-ray collimation, π^0 production target and detectors is essentially the same as previously reported. (Fig. 1.) The x-ray beam is collimated by lead collimators 6" thick inserted in a thick lead wall shielding the detecting apparatus from the stray

*Now at Stanford University.
**Now at Columbia University.

radiation from the synchrotron. The beam has a diameter of approximately 1-1/2" at the point where it strikes the π^0 production target. The detection apparatus consists of two "γ-ray telescopes," each telescope consisting of a set of three crystal counters. The crystals are stilbene units of size 5/8" x 1-3/4" x 1-3/4", mounted in light shields with one of their narrow sides facing a 1P21 photomultiplier. Each telescope consists of the following sequence:

(a) anti-coincidence crystal

(b) converter

(c) coincidence crystal

(d) absorber (usually omitted)

(e) coincidence crystal

An event constitutes a "count" if, in each of the two telescopes, the crystals (c,e) respond to a particle at minimum ionization or more and (a) does not.

A block diagram of the electronics is shown in Fig. 2. The coincidences and anti-coincidences are made in multivibrator circuits of about 10^{-7} sec resolving time developed by L. Wouters. Each telescope is again put in coincidence with the other, both with a similar circuit as well with a fast (10^{-8} sec) distributed amplifier coincidence circuit developed by C. Wiegand and described elsewhere.[6] The accidental coincidence rate is defined by the resolution of this single fast coincidence unit; the coincidence counting rate of each separate telescope corresponds to real events.

Fig. 3 shows a curve of quadruple coincidence counting rate as a function of photomultiplier gain. These and similar curves showed that operation took place on a reasonable plateau.

In our previous paper[1] we have discussed the arguments underlying the identification of the quadruple coincidence counts with γ-γ coincidences from the decay of a π^0. This argument is essentially as follows:

(a) The particles counted in each telescope are non-ionizing initially but are converted into ionizing radiation at the converter.

(b) Data on the conversion as a function of converter thickness and converter material are in agreement with the initial non-ionizing radiation being γ-rays but not neutrons.

(c) The range of the ionizing conversion products (for details, see Section C), shown to be electrons, corresponds to a γ-ray energy of the correct magnitude in agreement with the disintegration kinematics of a π^0 of mass $\sim$135 Mev into two γ-rays.

(d) The resultant spectra as a function of the correlation angle ϕ, notably the existence of a minimum correlation angle ϕ_c (see Section C), is in agreement with the kinematical relationship appropriate to π^0 disintegration.

In evaluating absolute cross sections, the efficiency of the detector must be evaluated and also the beam must be monitored absolutely. The detection system is such that a γ-ray will be detected if it produces at least one electron which (a) has enough range to penetrate to the second crystal after ionization and radiation loss, and (b) has not scattered out. The efficiency on this assumption is approximately calculable as a function of converter thickness and of γ-ray energy. Figs. 7 and 8 show the calculated efficiency as a function of converter thickness in one or both of the telescopes, respectively. These are compared with the experimental transition curves taken at $\phi = \theta = 90^\circ$. The corresponding γ-ray energy under this condition is nearly constant and of order 100 Mev. Fig. 9 shows the calculated efficiency as a function of γ-ray energy, for a 1/4" lead converter. Note that the efficiency drops very rapidly for small γ-ray energies; this is due to the decrease in pair cross sections in conjunction with the requirement as to minimum range of at least one of the electrons.

The average of the γ-rays to be detected lies above half the π^0 rest energy. The reason is that solid angle considerations favor those disintegrations in which the γ-rays are Doppler shifted toward higher energy. A value for the mean efficiency of .50 is thus not unreasonable.

The x-ray beam of the synchrotron was monitored by an integrating ionization chamber placed ahead of the collimator in the fringing field of the synchrotron. This chamber was calibrated by the method of Blocker, Kenney and Panofsky[7] and was recalibrated occasionally during these measurements. The authors are indebted to Messrs. Blocker and Kenney for carrying out these recalibrations. It is believed that the absolute energy flux of photons through the target is known to better than ± 20 percent.

C. Kinematics

Let ϕ be the angle subtended between the telescopes at the target. Let Θ be the angle between the direction of the beam and the plane defined by the telescopes and the target.

If we assume that the coincident gamma rays are due to π^0 mesons disintegrating into two photons, then several kinematical relations governing the process can be derived. If θ_0 is the angle between the gamma ray pair and the direction of motion of the π^0 measured in the frame of the π^0, then:

$$\sin(\phi/2) = \gamma^{-1}/(\gamma^{-2}\cos^2\theta_0 + \sin^2\theta_0)^{1/2} \qquad (1)$$

where $\gamma = E/E_0 = 1/(1 - \beta^2)^{1/2}$ is the ratio of total relativistic energy to rest energy of the π^0. For a given energy no gamma rays should be observed at any angle less than that given by $\sin(\phi_c/2) = \gamma^{-1}$.

Fig. 4 shows a plot of ϕ_c vs. γ. The probability $P(\phi)d\phi$ of observing a γ-ray pair corresponding to a π^0 velocity β between a correlation angle ϕ and $\phi + d\phi$ is given by (using the fact that the γ-ray emission in the frame of the π^0 is isotropic):

$$P(\phi)d\phi = \sin\phi \; \frac{1}{(1 - \mu)^{3/2}} \; \frac{d\phi}{\beta\gamma\sqrt{(1 - \mu)\gamma^{-2} - 2}} \qquad (2)$$

where $\mu = \cos\phi$. This function is shown in Fig. 5 for several values of γ. It should be noted that the probability is highest near the critical correlation angle ϕ_c and hence we have a near one-to-one correspondence between observed correlation angle and

π^0 velocity. This one-to-one correspondence is of course not exact; for a distribution of velocities the probability $P(\phi)$ will be an integral of (2) over a range of velocities from the lowest value permitted for a given ϕ to the highest value energetically possible.

The counting rate of a given counting geometry can be analyzed by treating the problem as if the coincidence resulted from the correlation probability (2) without any further reference to the π^0 motion proper.

Let $\Delta\Omega_1$ and $\Delta\Omega_2$ be the solid angle subtended by the limiting aperture of each telescope at the production target.

Let $N(\gamma)d\gamma d\Omega$ be the probability that a π^0 be emitted between energy γ and $\gamma + d\gamma$ into a solid angle $d\Omega$.

The probability of a coincidence count is then:

$$C(\phi) = 2\int_{\gamma_c}^{\gamma_{max}} P(\phi)d\phi \; N(\gamma)d\gamma \cdot \Delta\Omega_1 \cdot \frac{\Delta\Omega_2}{2\sin\phi d\phi}$$

$$= \frac{\Delta\Omega_1\Delta\Omega_2}{\pi}\int_{\gamma_c}^{\gamma_{max}} \frac{N(\gamma)d\gamma}{\beta\gamma\sqrt{(1-\mu)\gamma^{-2}-2}} \qquad (3)$$

Here $\gamma_c = \sqrt{2/(1-\mu)}$ is the lower limit of energy corresponding to a given μ and γ_{max} is the energetic upper limit of the production process.

Eq. (3) constitutes an integral equation between the counting rate and the π^0 production probability as a function of energy. Its inversion will be discussed later. Note that for a given value of the detector plane angle θ (see Fig. 1), the integral (3) averages over a small range of π^0 production angles; only in the case $\theta = \pi/2$ is the production angle fixed. However, for the range of angles used this fact will be ignored and the detector plane angle will be identified with the π^0 production angle.

The curve of efficiency vs γ-ray energy (Fig. 9) gives rise to a discriminatory effect on the energy spectrum of the π^0's, as calculated from the angular correlation

curves by means of Eq. (3). The reason is that near $\phi \approx \phi_c$ both γ-rays will have high energy and thus be detected efficiently, while near $\phi \sim 180^\circ$ one of the two γ-rays will have low energy if the π° energy is large. Hence the one-to-one correspondence between the correlation angle ϕ and the π° energy is actually even better than that implied by the integrand of Eq. (3).

D. Range of Conversion Electrons from γ-Rays

Fig. 6 shows the geometrical arrangement used in measuring the range of the conversion electrons. Space did not permit using beryllium absorbers entirely; for greater ranges than 22 g/cm^2 Be, a mixture of Be and Cu absorbers was used. The radiation straggling is thus not as small as it could be. The data were taken at $\theta = 70^\circ$, $\phi = 90^\circ$ with 1/16" Pb converter in the arm of the telescope containing the absorber. Fig. 7 shows a plot of the counting vs the g/cm^2 of absorber in one of the arms of the telescope in Fig. 6. For a correlation angle of $\phi = 90^\circ$ the mean π° velocity is $\beta = .73$; hence the energy per γ-ray is $1/2\ E_o/\sqrt{1-\beta^2} = .73\ E_o$. The observed mean electron energy of the more energetic of the pair electrons is 80 ± 12 Mev; the corresponding γ-ray energy is essentially 4/3 of this amount, or, using the more exact pair energy division probabilities, 110 ± 17 Mev. Hence, $E_o = 150 \pm 23$ Mev, in excellent agreement with the measurements obtained from the γ-ray spectrum from the charge exchange absorption of the π^- meson.[2]

E. Photoproduction in Beryllium.

A series of runs was made studying the yields of photo mesons from beryllium. These measurements constitute improvements over the work previously reported.[1] The target was a Be cylinder with its axis perpendicular to the plane defined by the telescopes, 1-1/2" long and 4-1/2" diameter; the beam diameter at the target was 3/4". The telescopes were positioned such that the farthest crystal was at a distance of 7" from the center line of the Be cylinder. The converters used were lead sheets of 1/4" thickness and 1-1/2" x 3" in size. The limiting aperture is thus the last crystal which is approximately 1-3/4" x 1-3/4" in size.

Fig. 11 shows the observed correlation curves. These were taken at three values of the angle θ. Table I shows a typical tabulation of the counting rates observed in the various channels.

Counts per 8.3×10^8 effective quanta			
θ / φ	45°	90°	135°
180°	.59	.59	.59
150°	1.66	.81	.97
120°	2.48	2.58	1.71
105°	5.28	3.44	1.83
90°	8.65	5.46	1.87
82-1/2°	10.5	--	--
75°	10.4	4.1	1.14
67-1/2°	9.9	--	--
60°	5.4	.95	.12
45°	1.26	.21	--

Table I

Tabulation of Coincidence Counting Rates Corresponding to π^0 Photoproduction in Beryllium

The qualitative picture as to the π^0 disintegration kinematics underlying these spectra is well confirmed. Note that the minimum angle decreases in the forward direction due to the increased upper limit of meson energy.

The observed correlation curves enable us to evaluate the energy distribution of the π^0 mesons approximately. Eq. (3) constitutes an integral equation for the energy distribution. The $\theta = 90^\circ$ curve would yield the energy distribution of π^0 mesons emitted at 90°. The curves at other values of θ correspond to π^0 trajectories in the plane defined by the counters and the target. Not all of these correspond exactly to emission at an angle θ; however, the deviation is small enough to be neglected here.

The integral equation can be inverted by formal methods. It turns out however that the accuracy of the observations is not sufficient to make effective use of such procedures. The most practical means of inversion is to assume that the true energy

distribution is "synthesized" out of a finite number (say N) of energy distributions constant over a given energy interval. If we assume such distributions to have arbitrary amplitudes A_N, then the A_N can be determined by fitting the observed correlation curve at N points and solving N linear equations. The correlation curve $\theta = \pi/2$ has been fitted by this means. The assumed distribution is shown in Fig. 12. Fig. 13 shows a comparison of the correlation curve calculated on the basis of the energy distribution of Fig. 12 and the experimental data. It is clear that although the observed correlation curves are not very sensitive to details in the energy distribution, they are sufficiently sensitive to give the relative amounts of low energy and high energy contributions in the distribution. The reason is that each high energy component will contribute intensity between the corresponding lower limiting correlation angle and 180°. Hence if the high energy components already account for the entire intensity at $\phi = 180^\circ$, then very little low energy components can be present. This, as shown in Fig. 12, is actually the case here. Fig. 14 shows in contrast the expected correlation curve if the π^0 energy distribution had been identical with the π^+ photo meson distributionas reported by Steinberger and Bishop.[8] Clearly the actual π^0 distribution rises more slowly from its limit than does the π^+ distribution. We shall discuss this point later.

A remark might be made here concerning the meaning of a cross section for these processes. If we define the number Q of "effective quanta"[9] or "McMillans" by:

$$Q = U/k_o \qquad (4)$$

where U is the total energy of the x-ray beam and k_o its upper energetic limit, then we can define a cross section per effective quantum (McMillan) directly in terms of the data as tabulated above. This is a consistent procedure, but one would prefer in the theoretical interpretation of most of these data to have a true cross section per photon at a definite photon energy. Such a cross section can be derived from this data approximately if we assume:

(a) That the one-to-one correspondence between correlation angle ϕ and the

meson velocity is exact, i.e., if the curves of Fig. 5 were δ-functions located at a mean correlation angle.

(b) That the production kinematics of the π^0 in various materials is the same as on a free nucleon, i.e., that there is a unique relationship between π^0 and primary photon energy.

We shall shortly obtain the absolute cross sections in these two interpretations.

The estimate of the absolute cross section per effective quantum can be made by use of the curves of Fig. 10. Let η = detection efficiency of each telescope; let $\Delta\Omega$ solid angle subtended by each telescope at the target. The number $P(\phi,\theta)$ of pairs counted is then:

$$P(\phi,\theta) = N(\phi,\theta)\left(\frac{\Delta\Omega}{2\pi\sin\phi}\right)(\Delta\Omega)\,\eta^2 \times 2, \qquad (5)$$

where $N(\phi,\theta)$ is the number of gamma pairs emitted per unit solid angle in θ and per unit plane angle in ϕ. We take $\eta = .50, \Delta\Omega = 0.063$. If the total number of quanta in the beam passing through the target of N atoms/cm^2 corresponding to the beam is Q, the cross section is thus:

$$\frac{d\sigma}{d\Omega} = \frac{3160}{NQ}\int P(\phi,\theta)\sin\phi\,d\phi$$

$$\sigma = \frac{3160}{NQ}\iint P(\phi,\theta)\,2\pi\sin\theta\sin\phi\,d\phi\,d\theta \qquad (6)$$

Numerical integration of the data of Table I gives:

θ	$\frac{d\sigma}{d\Omega} \times 10^{29}$ cm^2/effective quantum/steradian
45°	4.41
90°	3.13
135°	1.06

$\sigma = 3.7 \times 10^{-28}$ cm^2/effective quantum.

These are the cross sections per effective quantum; to obtain the cross section per quantum at a given energy, some further analysis is necessary: The number of

quanta in a primary x-ray energy interval dK is very closely given by:

$$dQ = Q(dK/K) \tag{7}$$

where Q has been defined above. The differential cross section/quantum/unit solid angle of π^o emission is thus:

$$\frac{d\sigma}{d\Omega} = \left(\frac{\pi \sin\phi \, d\phi}{\Delta\Omega}\right) \frac{P(\phi,\theta)}{NQ(dK/K)} \frac{1}{\Delta\Omega} \frac{1}{\eta^2}$$

$$= 3160/NQ \; P(\phi,\theta) \sin\phi \; K \frac{d\phi}{dK} \tag{8}$$

This can be evaluated if $d\phi/dK = \frac{d\phi}{d\gamma} \cdot \frac{d\gamma}{dK}$ is unique. $d\phi/d\gamma$ can be replaced by the derivative of the mean value of ϕ, averaged over the distributions $P(\phi)$ of the type plotted in Fig. 5. $d\gamma/dK$ can be calculated from the kinematics of photo collisions with single nucleons for a given value of incident photon energy.

If measurements are made at that given ϕ for each value of θ corresponding to the mean value of the correlation curve for a fixed primary photon energy at the particular θ, then this one set of measurements is sufficient to generate an angular distribution $\frac{d\sigma}{d\Omega}(\theta)$ at that value of photon energy underlying the choice of the ϕ's.

Table II shows the set of measurements made at values of ϕ to correspond to a primary photon energy of 260 Mev.

θ	ϕ	Counts per 8.3×10^8 Effective Quanta	$\frac{d\gamma}{dK}$	$\sin\phi \frac{d\phi}{d\gamma}$	$\frac{d\sigma}{d\Omega} \times 10^{29}$ cm^2/steradian
34°	70°	10.2 ± .6	.911	.755	4.66 ± .27
45°	75°	10.5 ± .5	.858	.900	7.64 ± .36
55°	80°	8.0 ± .4	.801	1.060	6.69 ± .33
67½°	82½°	7.9 ± .4	.728	1.150	7.36 ± .37
90°	90°	5.5 ± .26	.602	1.414	5.62 ± .26
112°	97½°	3.2 ± .24	.506	1.660	3.00 ± .22
135°	105°	1.8 ± .13	.444	2.000	1.35 ± .10
150°	115°	1.36± .16	.415	4.000	.676 ± .08

Table II. Angular Distribution of π^o Photoproduction in Beryllium. Entries are Calculated According to Eq. (8) with $N = 6.1 \times 10^{23}/\sin\theta$ atoms/cm^2 to take Account of the Obliquity of the Target. $d\gamma/dK$ is Computed from the Production Kinematics on Free Nucleons. Photon energy = 260 Mev.

Since the corresponding data for the angular distributions of π^0's, photoproduced in H, are not available at this writing, the question might be raised to what extent the data of Table II, plotted in Fig. 15, are representative of the angular distributions of π^0's produced on a free proton. Three effects would make the two distributions differ:

1. The Be cross section includes production both from protons and neutrons.
2. The internal motion of the nucleons in Be in combination with the steep excitation of the π^0 photoproduction process would favor π^0's produced from nucleons moving toward the x-ray source.
3. The exclusion principle would modify the distribution somewhat, since the energy available to the proton recoil is a function of the π^0 emission angle. This effect is not very significant since the nucleon retains its identity in π^0 emission.

In agreement with the analogous situation in the case of π^+ production[8] we therefore believe that the photoproduction of π^0 mesons would lead to a still more forward distribution than that given in Fig. 15.

The integrated cross section for 260 Mev photons 5.55×10^{-27} cm^2. Note that this is almost twice as large as the value quoted per effective quantum. This is quite reasonable since the excitation of the process rises quite slowly near threshold.

The absolute values quoted here should be accurate to a factor of two. Three significant figures are given to permit internal comparison. Probable errors refer to statistics only. Clearly the distribution is directed well forward in contrast to the corresponding curves for charged meson production.

F. Z Dependence of Production.

The Z dependence of π^0 production was studied by measuring the yield of gamma-gamma coincidences at $\theta = 45^\circ$ and $\phi = 75^\circ$. The results are tabulated below. The targets were either solid cylinders (C and Be) or the material inserted in bakelite

cylinders (Li, Al, Cu and Pb). Similar to the experimental difficulties in the work on the Z dependence of charged photomesons,[9] it turned out to be difficult to accumulate satisfactory statistics for heavy elements.

Material	g/cm^2	counts/monitor/nucleon	Number of counts observed
Li	2.71	.190 ± .012	365
Be	8.80	.148 ± .007	458
C	8.09	.145 ± .009	307
Al	1.51	.126 ± .012	129
Cu	.90	.077 ± .010	74
Pb	.39	.051 ± .020	20
H (see section G)		.208 ± .029	

Table III. γ-γ Coincidence Counts as a Function of Z of Target Material

The yield per nucleon is a decreasing function of Z. In fact, if the yield per nucleon is plotted against $A^{-1/3}$ a straight line is obtained. Fig. 16 shows a plot of the neutral meson yield per nucleon and a yield of the π^+ yield per proton (according to Mozley[9]) plotted against $A^{-1/3}$. Both sets of data are compatible with a straight line dependence. Since it appears thus that the yield is proportional to the nuclear surface and since the mean free path for photons in nuclear matter is large, we can conclude that the meson mean free path within the nucleus is not in excess of a small multiple of $\hbar/\mu c$. This is in agreement with the recent experiments on nuclear interaction of mesons.[10]

G. Yield from Hydrogen.

The data on the π^o yield from hydrogen are as yet incomplete and the data presented here must be considered preliminary. The hydrogen cross section has been measured by two methods: (a) subtraction method CH_2 (polyethylene) vs. C,

(b) production in liquid H_2.

(a) Subtraction Method.

The two targets employed in the subtraction method were constructed as follows:

1. CH_2 target - cylinder: height - 2.000"; diameter - 1.627"; weight - 62.97g; total surface density - 4.70 g/cm^2; carbon surface density - 4.03 g/cm^2.
2. C target - cylinder constructed of 1/16" graphite layers perforated by 1/8" holes in random fashion: height - 1.947"; diameter - 1.630"; weight - 54.16 g; surface density - 3.94 g/cm^2.

The carbon target thus represents the carbon content of the CH_2 target to a fair degree of approximation.

Data were observed with the telescopes set at $\theta = 90^\circ$, $\phi = 90^\circ$. The results are tabulated below.

	CH_2	C	Difference
Total count	1157	911	
Accidentals	44	59	
Net count, corrected to equal carbon content	1098	885	213 ± 45

Table IV

We obtain thus:

$$\frac{\sigma_{90^\circ(\text{hydrogen})}}{\sigma_{90^\circ(\text{carbon})}} = .120 \pm .025$$

Assuming that the correlation functions for H and Be are similar we obtain an estimate for the total cross section:

$$\sigma = .60 \times 10^{-28} \text{ cm}^2/\text{effective quantum at 320 Mev.}$$

Due to the difficulty in obtaining adequate statistics with a subtraction method, no data on the angular distribution and correlation function were taken.

(b) Liquid H_2 Target.

The target used was constructed by Leslie Cook of this Laboratory[11] and the authors are greatly indebted to him for permission to use the instrument. The target essentially constitutes a line source of two inches diameter. This line source was surrounded by a lead cylinder 1" thick. A slit cut into the cylinder defined the effective length of the line source. Since the geometry of the hydrogen target made a large distance from the target to the counters necessary, larger counters were required to maintain a sufficient solid angle. These counters were made of cylindrical pyrex containers 4" in diameter and 1" in height filled with a solution of terphenyl in xylene. 1P28 photomultipliers were used to "look" at the solution through a 1 mm thick pyrex window sealed onto the edge of the vessel. This system leads to a fairly non-uniform light signal as a function of position of a fast electron track; hence very high photomultiplier gains were required to operate on a plateau. This leads of course to an unfavorable ratio of singles to doubles count and hence of accidental coincidences to real events. With this exception, the arrangement and the electronics were as described above and as previously reported.[1]

Data were taken with and without liquid hydrogen in the hydrogen target. The background due to the empty target averaged 30 ± 5 percent. Statistics were insufficient to justify point-by-point correction of the observed data. A correction factor of .70 ± .05 was thus applied to the hydrogen data. Table V shows the data observed. These data are plotted in Fig. 17. We can again use these data to estimate an absolute cross section. Using $\Delta\Omega = .1$; $\eta = .50$; effective source length = 5.0 cm, we obtain, since:

$$\frac{d\sigma}{d\Omega}(\theta) = \frac{\pi}{NQ\eta^2}(\Delta\Omega)^2 \int_0^{\pi} P(\phi,\theta)\sin\phi d\phi = 4.3 \times 10^{-30} \int P(\phi,\theta)\sin\phi d\phi$$

$\text{cm}^2/\text{steradian/effective quantum}$ (9)

Hence:

$$\frac{d\sigma}{d\Omega}(90^\circ) = 3.5 \times 10^{-30} \text{ cm}^2/\text{steradian/effective quantum}$$

$$\frac{d\sigma}{d\Omega}(45^\circ) = 8.2 \times 10^{-30} \text{ cm}^2/\text{steradian/effective quantum}$$

The total cross section can then be estimated to be $.55 \times 10^{-28}$ cm^2/effective quantum, in good agreement with the result derived from the subtraction method.

ϕ	θ	count/1.39×10^9 effective quanta
48°	90°	$.11 \pm .04$
$67\frac{1}{2}^\circ$	90°	$.76 \pm .07$
90°	90°	$.89 \pm .09$
112°	90°	$.25 \pm .04$
135°	90°	$.17 \pm .03$
157°	90°	$.06 \pm .03$
67°	45°	$3.96 \pm .30$
90°	45°	$1.14 \pm .10$
135°	45°	$.38 \pm .07$
157°	45°	$.35 \pm .07$

Table V. Correlation Curves for γ-γ Coincidences from Liquid Hydrogen.

The data of Fig. 16 are very similar to the beryllium data of Fig. 10. A step distribution fitting the hydrogen data is shown in Fig. 17. We can therefore conclude definitely that the excitation function for π^0 produced by photons has a higher order contact as compared to the production of charged photo mesons.

These data are in agreement as to excitation function with the data reported by Silverman and Stearns.[12] Silverman and Stearns obtain the excitation function in a somewhat more direct manner by measuring the coincidence yield between the recoil proton and one of the two gamma rays. They confirm the form of the excitation curve and their absolute cross section agrees with ours.

G. Discussion.

In their more elementary and "non-controversial" interpretation these data principally add to the phenomenology of neutral mesons. The experiments show again that a particle of rest energy of the order of 135 Mev disintegrates into

two and only two photons. The particles are of strong nuclear interaction as evidenced by their internal nuclear absorption. The lifetime of the particles is sufficiently long that they are definitely "real," i.e., the decay takes place outside the nuclear field. These properties define the particle and show it to be almost certainly identical with the π^0 inferred from the experiments in high energy nucleon collision in the laboratory and in cosmic rays and identical to the product of charge exchange scattering of charged π^- mesons.

The two γ decay fixes the spin of the π^0 meson as zero or an integer greater than or equal to 2.

In addition to yielding information on the property of the particle itself, these experiments give data on the photoproduction process of π^0 mesons. The more obvious features of the process are:

1. The cross section on nucleons is of the same order; in fact roughly one-third of the production process for positive charged mesons.
2. The excitation function of the π^0 production exhibits a higher order contact near threshold as compared to charged photomeson production. This fact and the absolute cross section is in agreement with the work of Silverman and Stearns.[12]
3. The angular distribution for π^0 photo mesons at a given photon energy is strongly peaked forward, in contrast to the π^+ data.
4. The Z dependence of production, other than for exclusion principle effects, of π^0 and π^+ are in agreement.

Because of the similarities between charged and neutral mesons in many respects and also because of the experimental evidence concerning charge independence of nuclear forces, it appears worthwhile to review the relation of these experimental results with the prediction of charge symmetrical meson theory. We shall discuss here only results based on considering the meson to have spin zero and odd intrinisic parity (pseudoscalar); we are thus excluding the possibilities of spin greater than 1.

The mode of π^0 decay precludes spin 1 and recent experimental evidence[13,14] on the reaction $\pi^+ + D \rightleftarrows p + p$ makes the value zero for the π^+ spin a certainty. An even parity spin zero (scalar) meson is ruled out by the results on absorption of π^- mesons in deuterium[2] and also by the photoproduction of π^+ mesons.[8]

In Table VI we list the principal calculations on photo meson production based on charge symmetric, pseudoscalar theory. These calculations were not offered as predictions but rather as possible explanations of these and other data as they became known. Perturbation calculation to order g^2 which had given results in good agreement with the π^+ photoproduction cross section failed to give satisfactory results here[15,16]; such a calculation fails to predict a sufficiently large cross section nor does it give the forward angular distribution observed. Carrying calculations to higher order[17] raises the cross section but also does not give the correct angular distribution. Furthermore it is difficult to take an expansion seriously whose second term exceeds the first and where an estimate of the discarded terms is lacking.

Meson-Nucleon Interaction	Nucleon-Electromagnetic Coupling	Type of Approximation Used.	Authors
pseudoscalar or pseudovector	no Pauli term	Perturbation theory to order g^2	Brueckner[15] Araki[16]
pseudoscalar	no Pauli term	Perturbation theory to order g^4	Brueckner and Watson[17]
pseudoscalar and pseudovector	Pauli term	Perturbation theory to order g^2	Kaplon,[18] Aidzu, Fujimoto, Fukudo[19]
pseudovector	no Pauli term	Strong coupling	Fujimoto and Miyazawa[20]
pseudovector	Pauli term	Classical	Breuckner and Case[21]
pseudovector	no Pauli term	Spin + charge classical	Drell[22]

Table VI

Kaplon[18] and Aidzu, Fujimoto and Fukudo[19] include the static anomalous magnetic moment of the proton explicitly in a second order calculation. This gives fair agreement with the absolute cross section, although the angular distribution is still in disagreement with the experimental results. This procedure, as has been pointed out by the authors themselves, is at best an arbitrary one; if the overall systematics of meson theory were correct, the effect of the anomalous moment, which is in itself a consequence of the interaction of the nucleon with the meson field, would automatically be taken care of in the calculation if it could be carried consistently to 4th order. It is only the difficulties of a consistent meson theoretical calculation of the moments which motivates this phenomenological approach.

Perhaps more interesting is the discovery[20,21] that the isobaric state of the nucleons which is characteristic of strong coupling theory gives rise to resonances in the photoproduction of mesons. This has been shown in the classical[21] and strong coupling[20] approximation. Assuming an isobaric state of excitation 250-300 Mev, rough agreement with all the π^0 production data presented here results. The phenomenological magnetic moments, however, are also used here. At the same time the predicted resonance in the π^+ spectrum is probably contrary to the experimental data.[8] There exists therefore at present no theoretical study of π^0 photoproduction which is free from logical inconsistencies and which fits all the experimental data as they are known at present.

H. Acknowledgements

This work has been executed with the cooperation of many members of this Laboratory. The authors are particularly indebted to the synchrotron crew under the direction of George McFarland for their efficient cooperation. Mr. Alex Stripeika assisted in the maintenance of the electronics. In its later phases Mr. Calvin Andre and Mr. John Foster assisted in the execution of the experiment. Finally the authors would like to express their appreciation to Professor Edwin McMillan for his active interest in this experiment. This work was performed under the auspices of the Atomic Energy Commission.

References

1. J. Steinberger, W. K. H. Panofsky, and J. Steller, Phys. Rev. 78, 802 (1950). References to earlier evidence concerning the π^0 given in this paper.

2. W. K. H. Panofsky, R. L. Aamodt, J. Hadley, Phys. Rev. 81, 565 (1951).

3. A. Sachs and J. Steinberger, Phys. Rev. 82, 973 (1951).

4. R. Hales, R. Hildebrand, R. Madey, W. Crandall, N. Knable, B. Moyer, private communication, and Phys. Rev. 83, 206 (1951).

5. Carlson, Cooper, and King, Phil. Mag. 41, 701 (1950).

6. Clyde Wiegand, Rev. Sci. Instr. 21, 975 (1950).

7. Blocker, Kenney and Panofsky, Phys. Rev. 79, 419 (1950).

8. J. Steinberger and A. Bishop, Phys. Rev. 78, 494 (1950).

9. R. F. Mozley, Phys. Rev. 80, 493 (1950).

10. See e.g., Bernardini, Booth, Lederman, Phys. Rev. 83, 1277, (1951). M. Camac, et al, Phys. Rev. 83, 1075 (1951); Phys. Rev. 82, 745 (1951). H. Bethe and R. Wilson, Phys. Rev. 83, 690 (1951).

11. Leslie Cook, UCRL-990, November, 1950.

12. A. Silverman and M. Stearns, Phys. Rev. 83, 206 (1951).

13. D. Clark, R. Wilson and A. Roberts, Phys. Rev. 83, 649 (1951).

14. R. Durbin, H. Loar, and J. Steinberger, Phys. Rev. 83, 646 (1951).

15. K. Brueckner, Phys. Rev. 79, 641 (1950).

16. G. Araki, Progress of Theoretical Physics VI, No. 4, 507 (1951).

17. K. Brueckner and K. Watson, private communication.

18. M. F. Kaplon, Phys. Rev. 83, 206 (1951).

19. K. Aidzu, Y. Fujimoto, H. Fukudo, Progress of Theoretical Physics VI, No. 2, 193, (1951).

20. Y. Fujimoto and H. Miyazawa, Progress of Theoretical Physics, No. 5, 1052 (1950).

21. K. A. Brueckner and K. M. Case, Phys. Rev. 83, 1141 (1951).

22. S. D. Drell, Phys. Rev. 83, 555 (1951).

Figure Captions

Fig. 1. Geometry of detection apparatus for observing γ-γ coincidences from π^0 disintegrations. The "correlation angle" ϕ and "telescope plane angle" θ (approximately the π^0 production angle) are indicated.

Fig. 2. Block diagram of electronics used in detecting γ-γ coincidences.

Fig. 3. Observed coincidence counting rate observed as a function of photomultiplier voltage. Within the rather poor statistics a plateau is indicated on this and similar runs.

Fig. 4. Plot of the minimum correlation angle ϕ_c against γ = ratio of meson kinetic energy/meson rest energy.

Fig. 5. Plot of $P(\phi)/\sin\phi$ (see Eq. (2)) against the correlation angle ϕ for three values of the meson energy. This function is the relative detection probability for a given correlated γ-ray pair.

Fig. 6. Disposition of scintillation cyrstals, lead converter and absorbers in the experiment attempting to determine the range of conversion electrons from the π^0 γ-rays.

Fig. 7. Absorption curve of conversion electrons as observed in the geometry of Fig. 6.

Fig. 8. Calculated and observed detection efficiency of the γ-ray pairs as a function of converter thickness in one telescope arm.

Fig. 9. Calculated and observed detection efficiency of the γ-ray pairs as a function of converter thickness in both telescope arms.

Fig. 10. Calculated detection efficiency of a telescope as a function of γ-ray energy.

Fig. 11. Relative coincidence counting rates as a function of correlation angle ϕ for three values of the telescope plane angle θ. Beryllium target.

Fig. 12. An energy distribution of π^0 mesons which would give rise to the γ-ray correlation curves of Fig. 11 for $\theta = 90^\circ$ in beryllium. The fit is made with six "square step" distributions of suitably adjusted amplitude.

Fig. 13. The smooth curve is the calculated γ-γ correlation curve under the assumption of the energy distribution of Fig. 12. The experimental data are given for comparison.

Fig. 14. Correlation curve which would have been expected if energy distribution of π^0 mesons were identical to the π^+ meson spectrum photoproduced from hydrogen at 90° as observed by Steinberger and Bishop.[8]

Fig. 15. Cross section per 260 Mev photon for π^0 production in beryllium as a function of production angle.

Fig. 16. Cross section of π^0 production per nucleon and cross section of π^+ production per proton according to Mozley[9] plotted against $A^{1/3}$ where A is the atomic number. Note that the yield varies linearly with nuclear area.

Fig. 17. Preliminary correlation curve for π^0 photoproduction in hydrogen. Shown are a) the experimental data, b) the curve (dotted line) of Fig. 14, expected if π^0 and π^+ photoproduction were identical and c) (solid curve) the correlation curve expected if the spectrum were the 4-step spectrum of Fig. 18.

Fig. 18. Step-energy spectrum compatible with the γ-γ correlation data from π^0 photoproduction at $\theta = 90^\circ$.

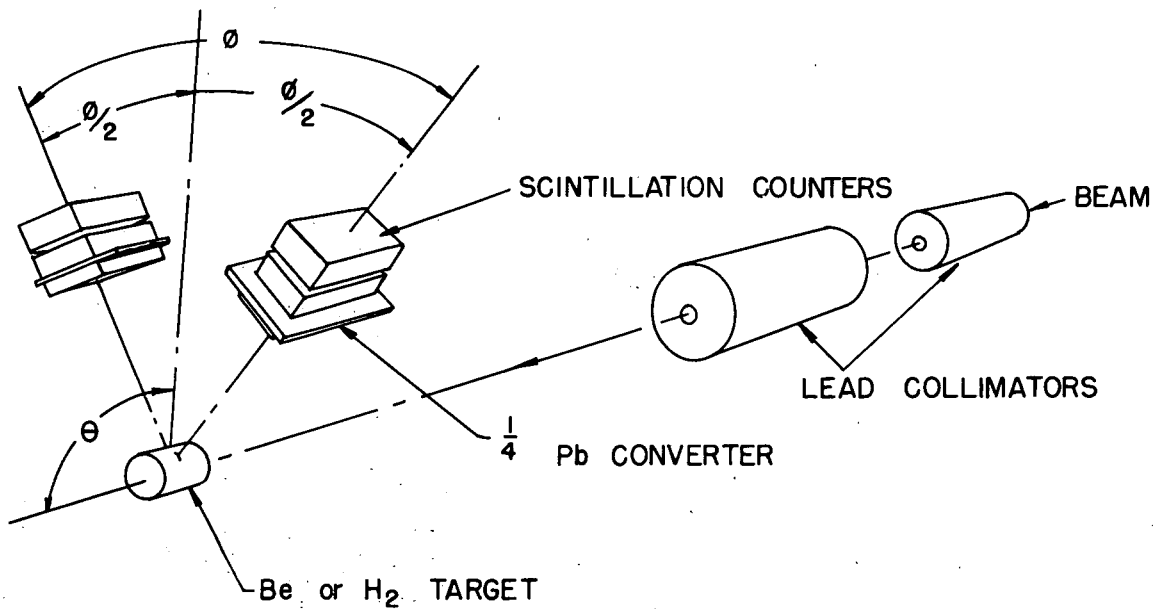
Ø
Ø/2
Ø/2
SCINTILLATION COUNTERS
BEAM
LEAD COLLIMATORS
θ
1/4 Pb CONVERTER
Be or H2 TARGET
MU 2731

Fig. 1

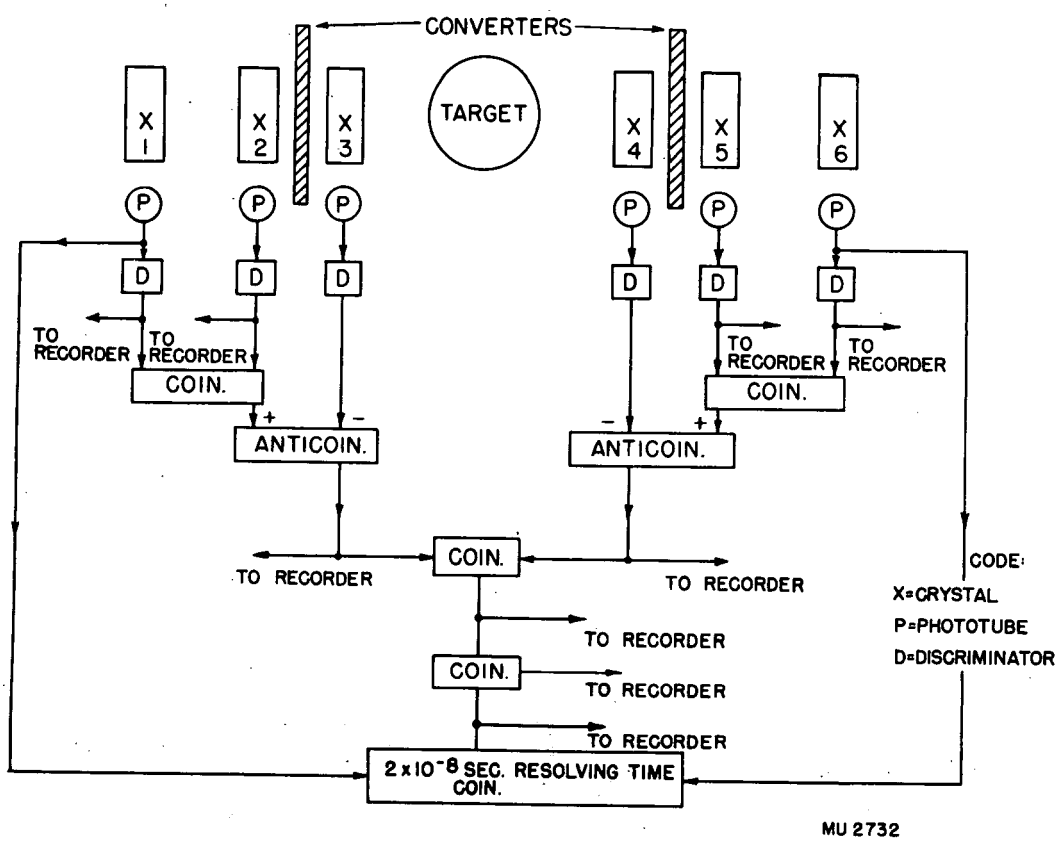
CONVERTERS
TARGET
X 1
X 2
X 3
X 4
X 5
X 6
P
D
TO RECORDER
COIN.
ANTICOIN.
+
−
CODE:
X=CRYSTAL
P=PHOTOTUBE
D=DISCRIMINATOR
2 x 10⁻⁸ SEC. RESOLVING TIME COIN.
MU 2732

Fig. 2

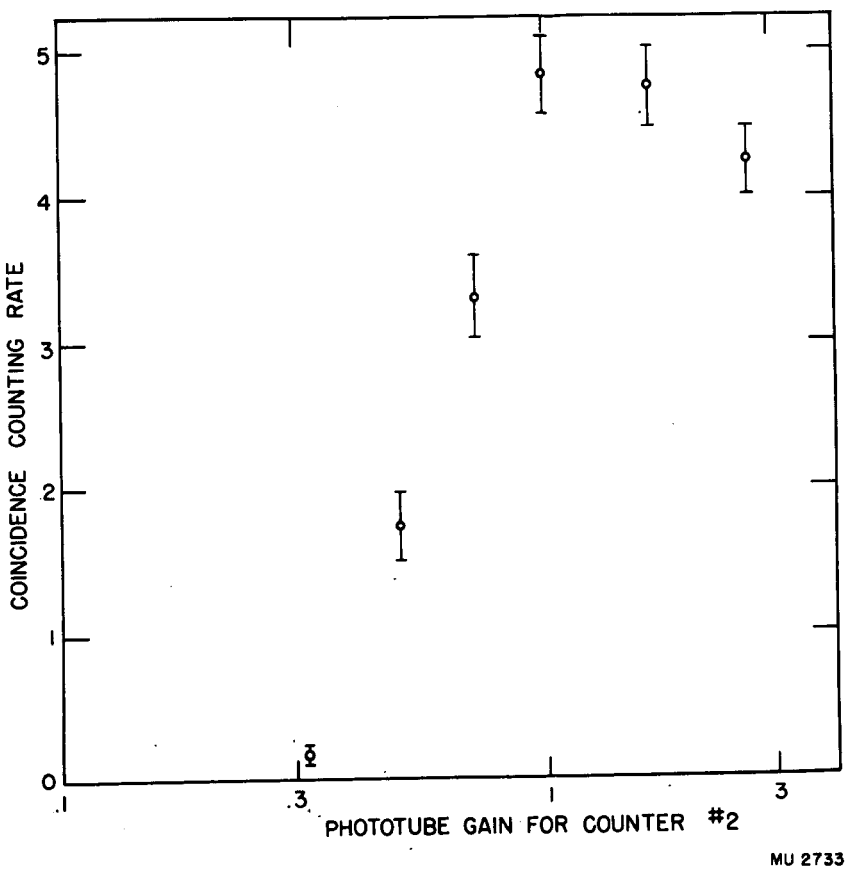
COINCIDENCE COUNTING RATE
0
1
2
3
4
5
.1
.3
1
3
PHOTOTUBE GAIN FOR COUNTER #2
MU 2733

Fig. 3

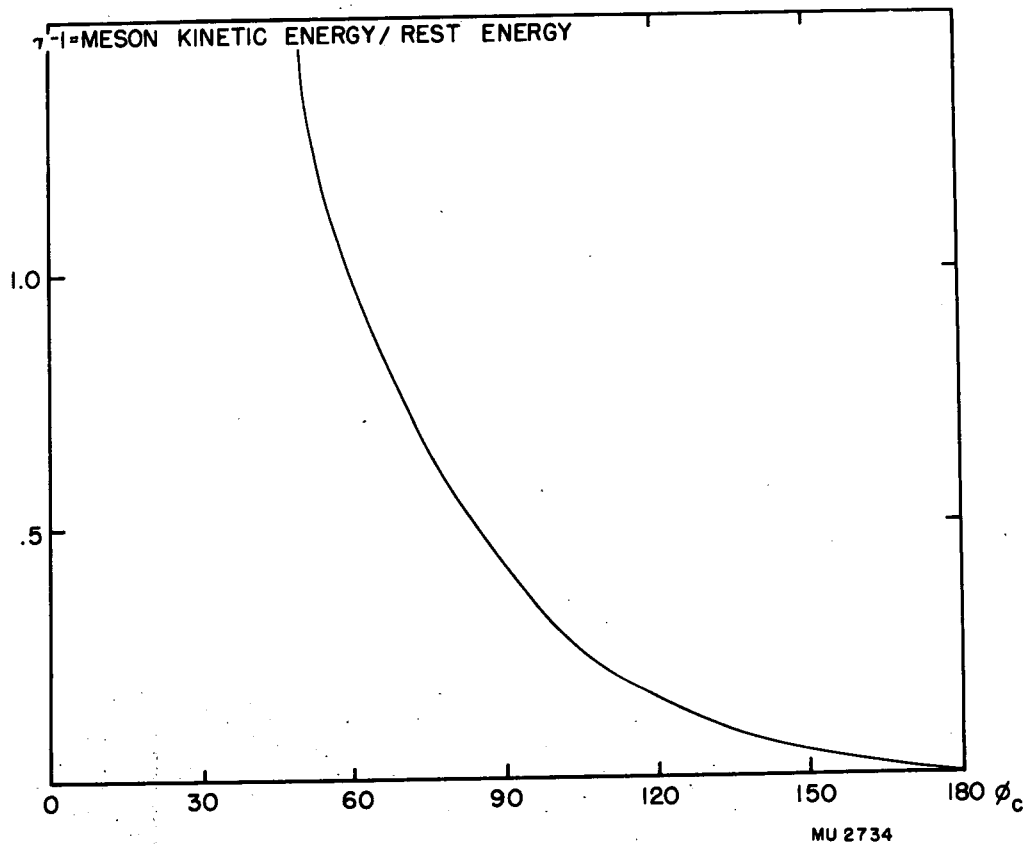
γ-1=MESON KINETIC ENERGY/ REST ENERGY
1.0
.5
0
30
60
90
120
150
180 φc
MU 2734

Fig. 4

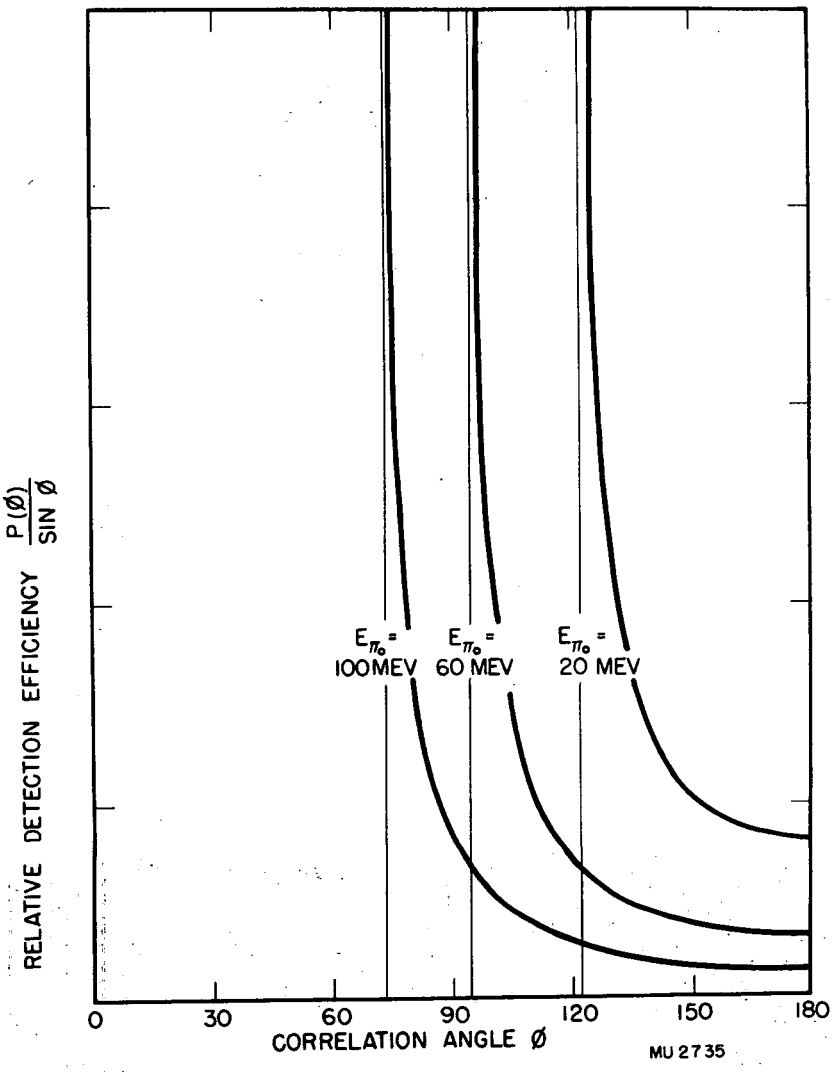
RELATIVE DETECTION EFFICIENCY P(Ø)/SIN Ø
E_{π_o} = 100 MEV
E_{π_o} = 60 MEV
E_{π_o} = 20 MEV
0
30
60
90
120
150
180
CORRELATION ANGLE Ø
MU 2735

Fig. 5

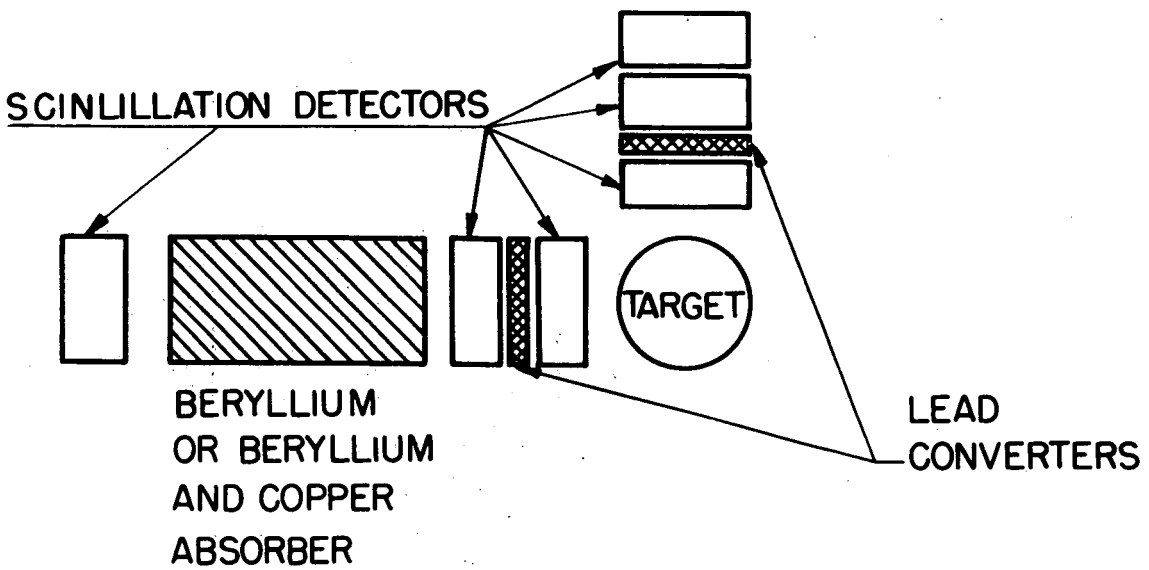
SCINLILLATION DETECTORS
TARGET
BERYLLIUM
OR BERYLLIUM
AND COPPER
ABSORBER
LEAD
CONVERTERS
MU2736

Fig. 6

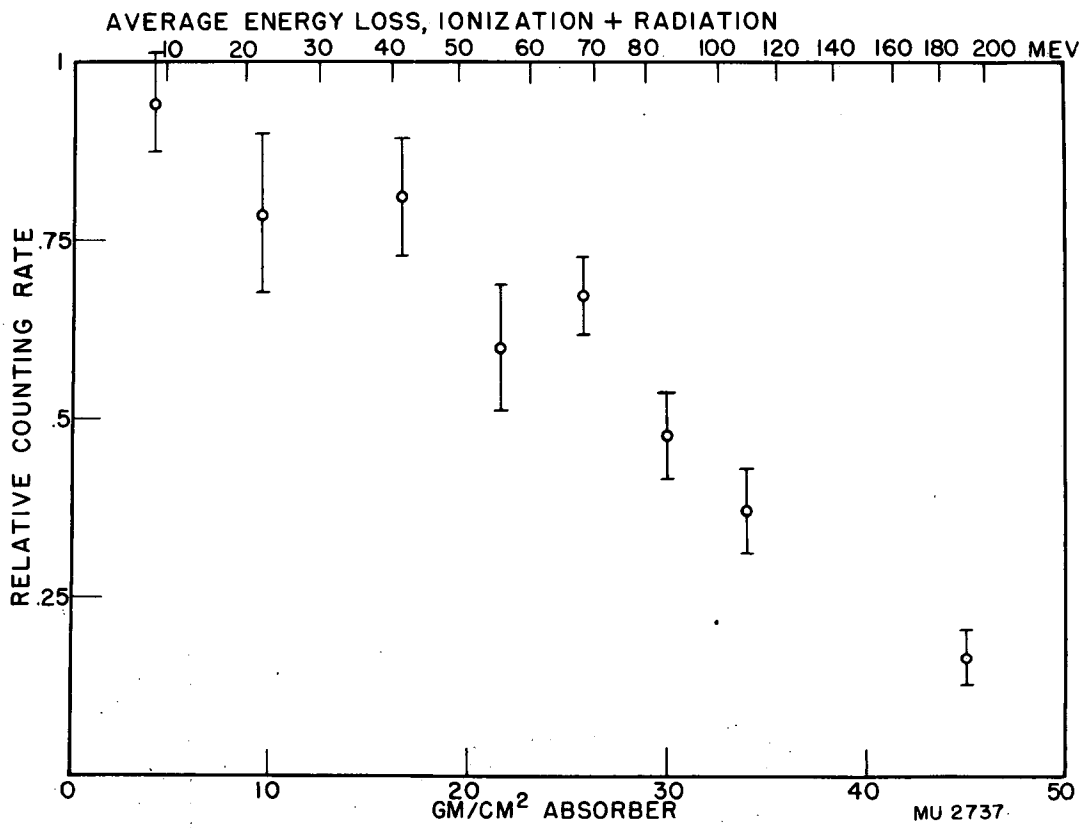
AVERAGE ENERGY LOSS, IONIZATION + RADIATION
10 20 30 40 50 60 70 80 100 120 140 160 180 200 MEV
RELATIVE COUNTING RATE
1
.75
.5
.25
0
10
20
30
40
50
GM/CM2 ABSORBER
MU 2737

Fig. 7

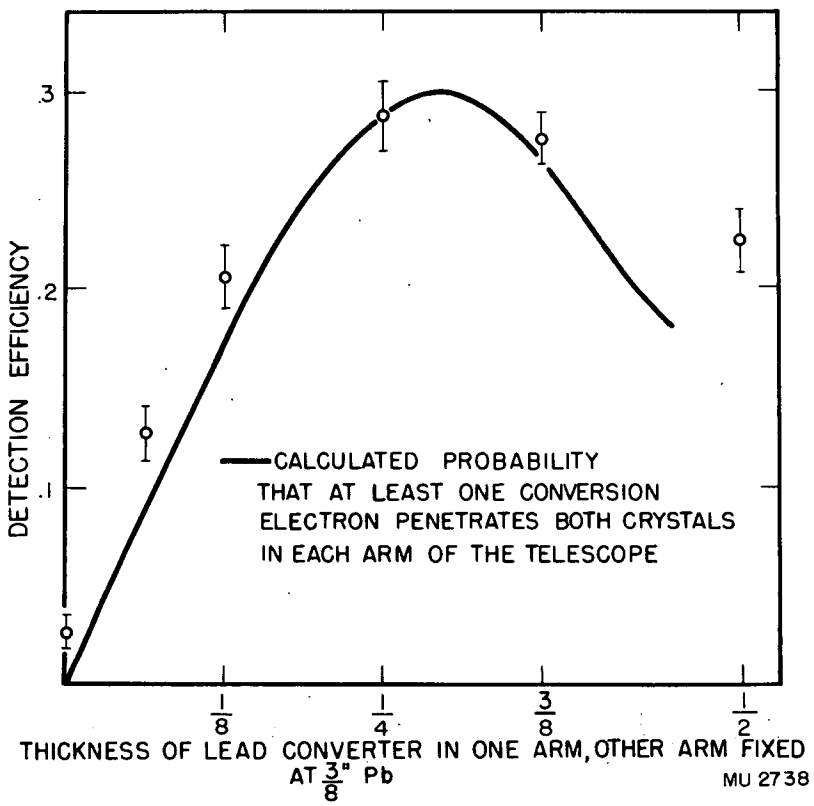
DETECTION EFFICIENCY
.3
.2
.1
CALCULATED PROBABILITY
THAT AT LEAST ONE CONVERSION
ELECTRON PENETRATES BOTH CRYSTALS
IN EACH ARM OF THE TELESCOPE
1/8
1/4
3/8
1/2
THICKNESS OF LEAD CONVERTER IN ONE ARM, OTHER ARM FIXED
AT 3/8" Pb
MU 2738

Fig. 8

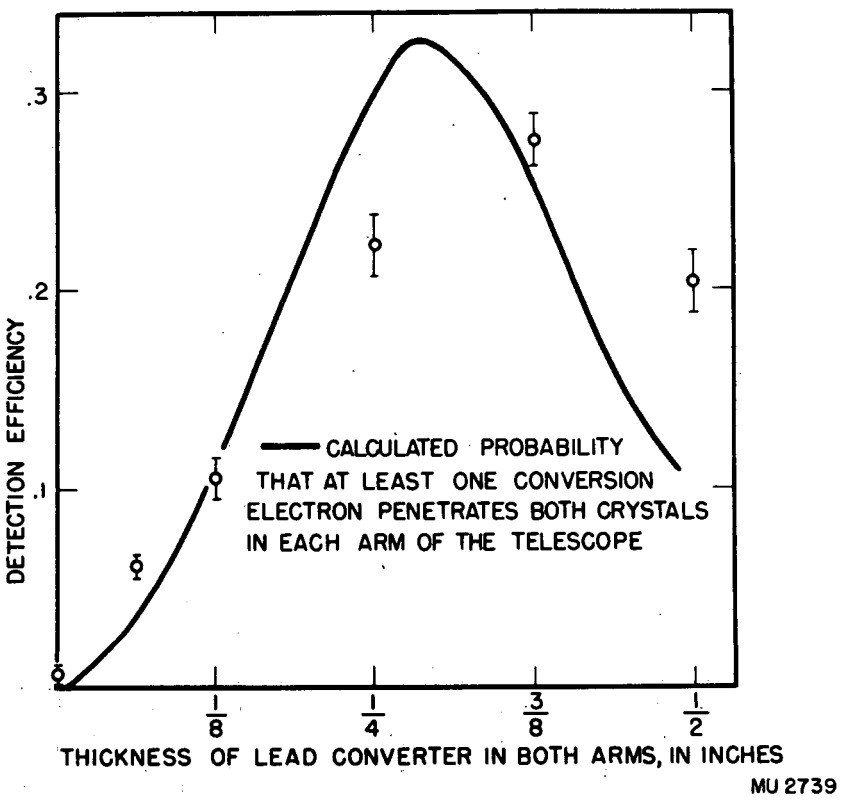
DETECTION EFFICIENCY
.3
.2
.1
CALCULATED PROBABILITY
THAT AT LEAST ONE CONVERSION
ELECTRON PENETRATES BOTH CRYSTALS
IN EACH ARM OF THE TELESCOPE
1/8
1/4
3/8
1/2
THICKNESS OF LEAD CONVERTER IN BOTH ARMS, IN INCHES
MU 2739

Fig. 9

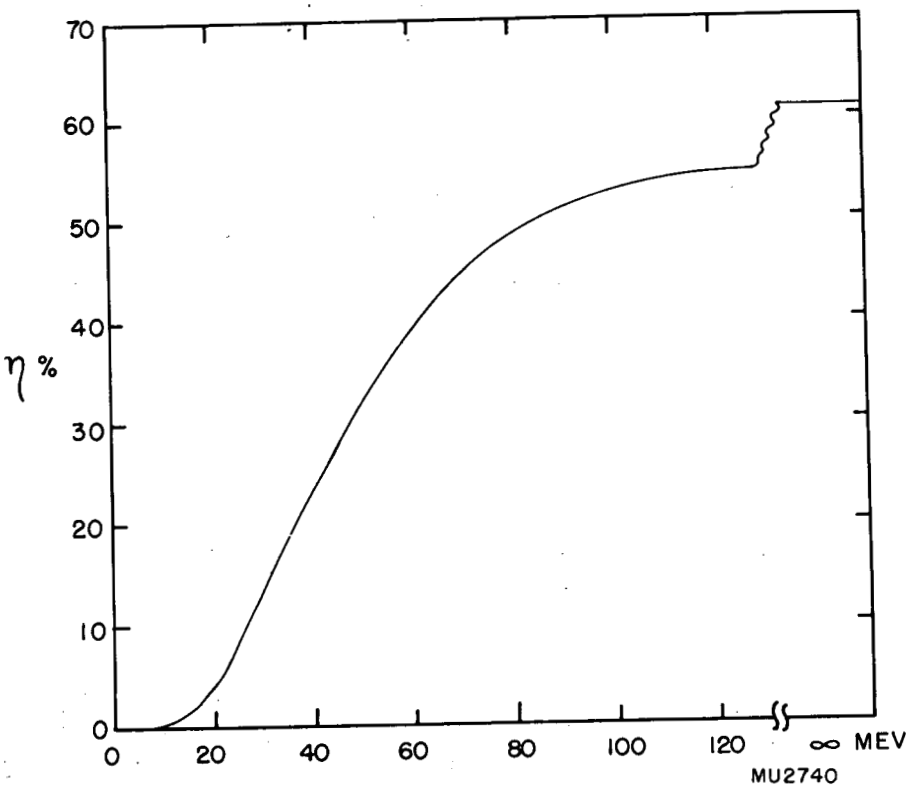

Fig. 10

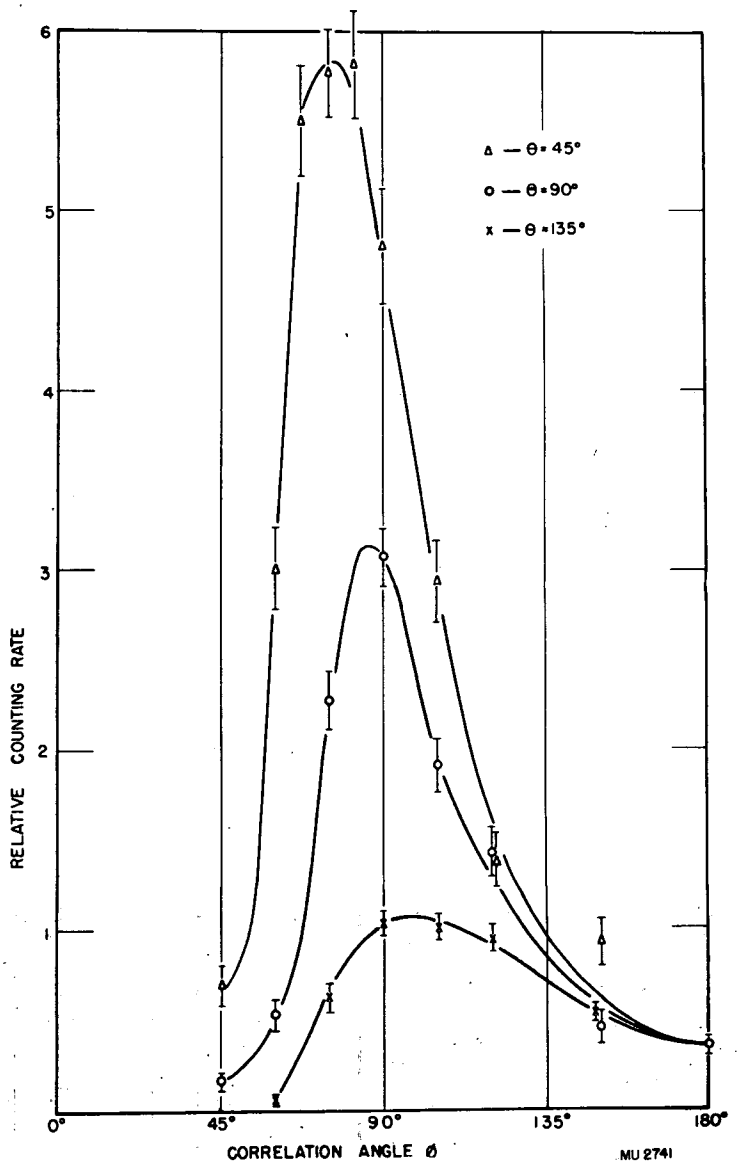
6
5
4
3
2
1
RELATIVE COUNTING RATE
Δ — θ = 45°
o — θ = 90°
x — θ = 135°
0°
45°
90°
135°
180°
CORRELATION ANGLE Ø
MU 2741

Fig. 11

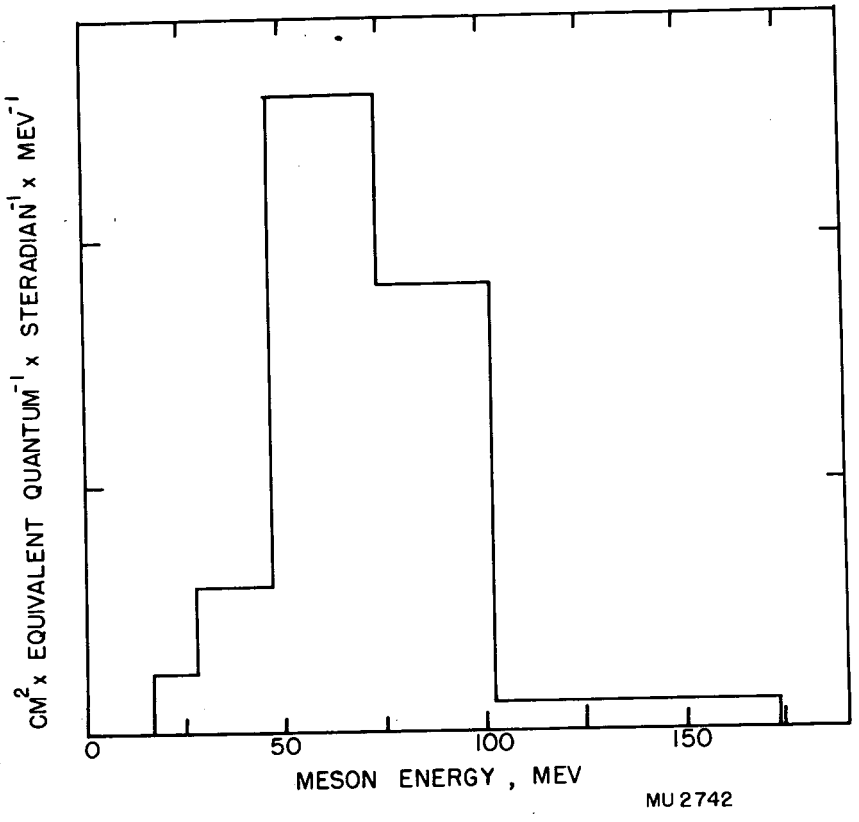
CM² x EQUIVALENT QUANTUM⁻¹ x STERADIAN⁻¹ x MEV⁻¹
0
50
100
150
MESON ENERGY , MEV
MU 2742

Fig. 12

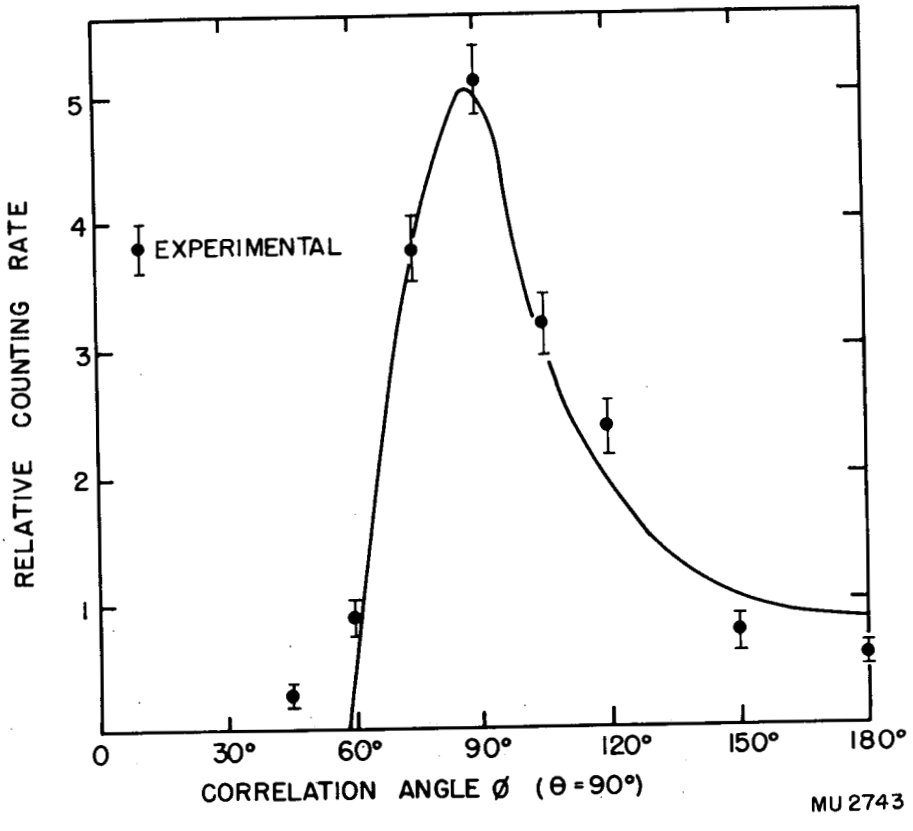
RELATIVE COUNTING RATE
EXPERIMENTAL
5
4
3
2
1
0
30°
60°
90°
120°
150°
180°
CORRELATION ANGLE Ø (θ = 90°)
MU 2743

Fig. 13

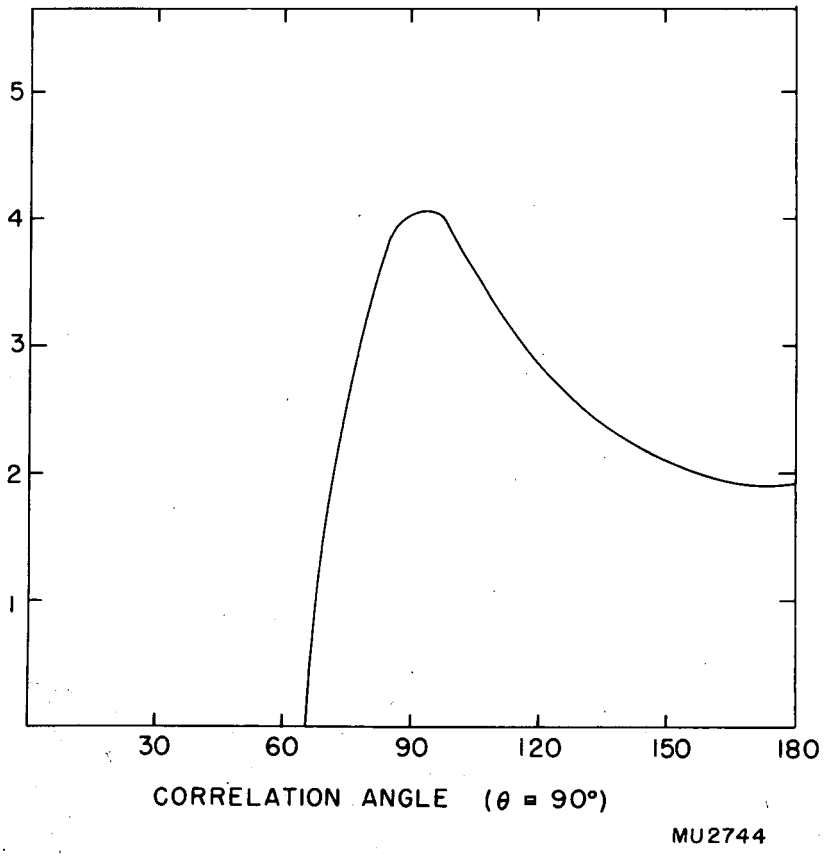

Fig. 14

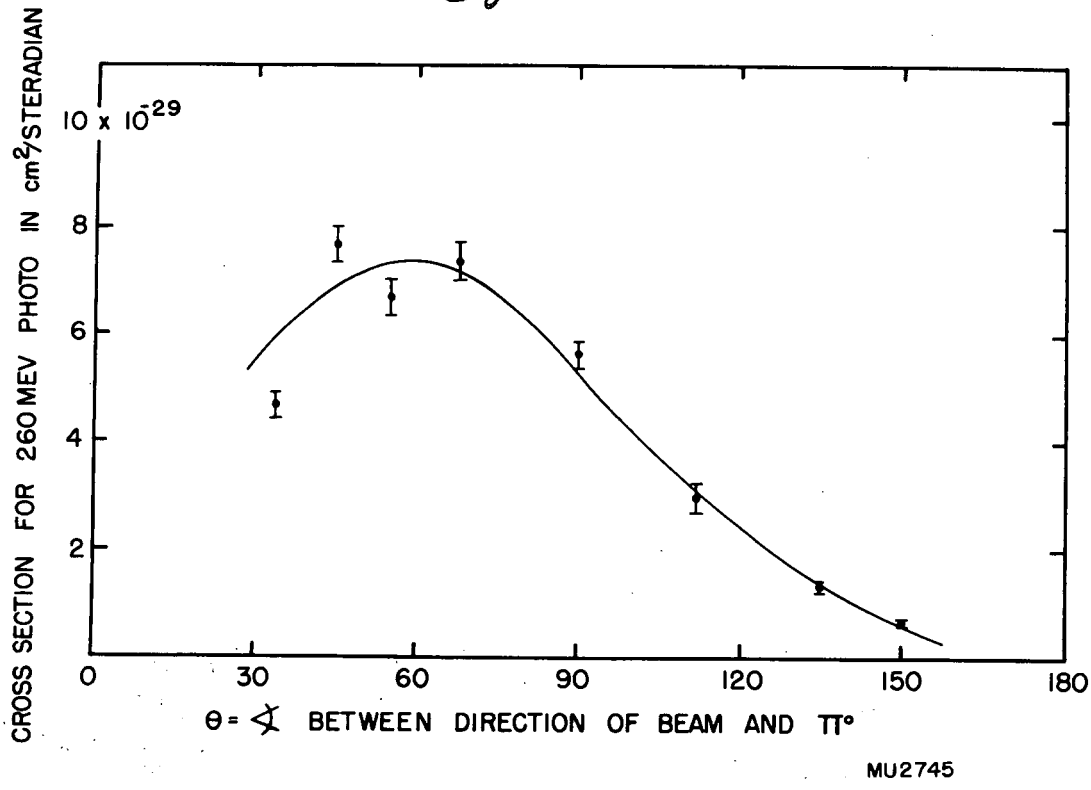
CROSS SECTION FOR 260 MEV PHOTO IN cm²/STERADIAN
10 x 10⁻²⁹
8
6
4
2
0
30
60
90
120
150
180
θ = ∢ BETWEEN DIRECTION OF BEAM AND TT°
MU2745

Fig. 15

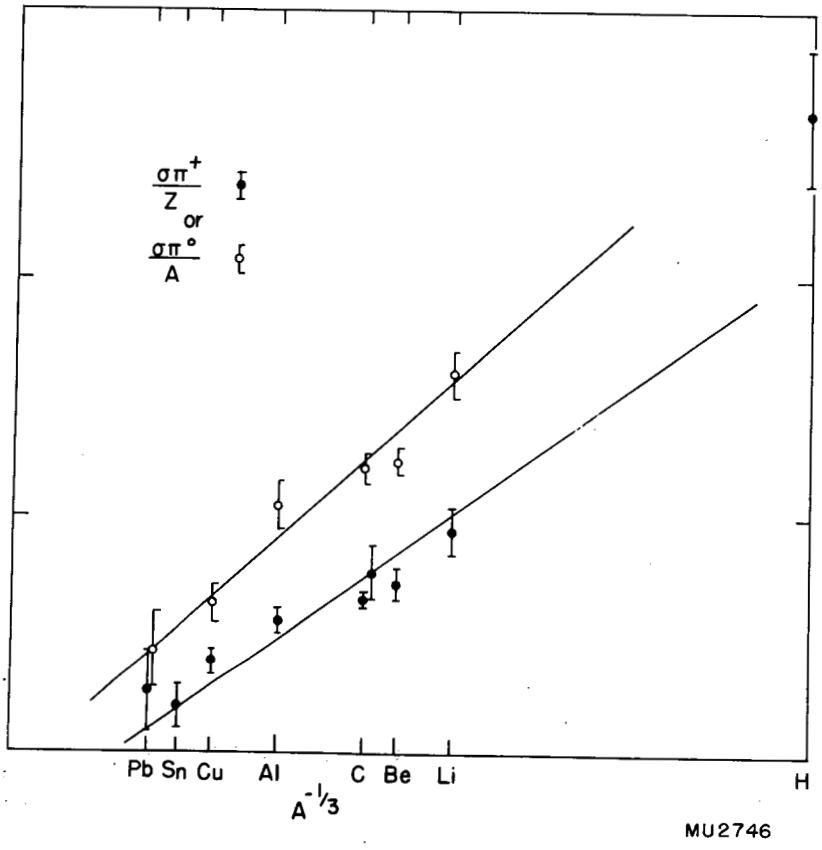

Fig. 16

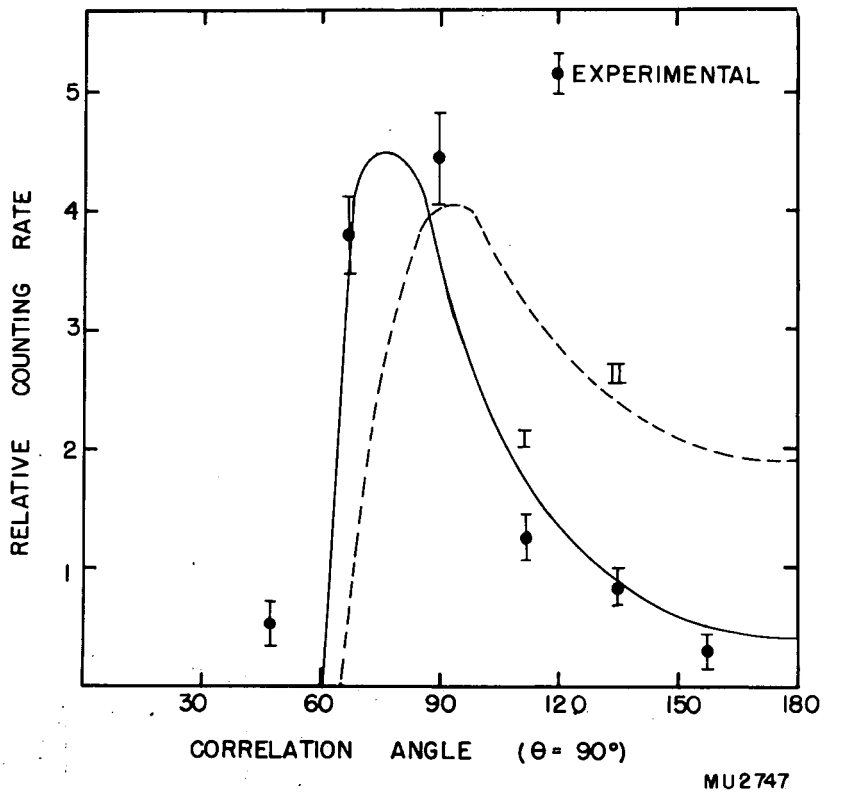
EXPERIMENTAL
RELATIVE COUNTING RATE
1
2
3
4
5
I
II
30
60
90
120
150
180
CORRELATION ANGLE (θ = 90°)
MU2747

Fig. 17

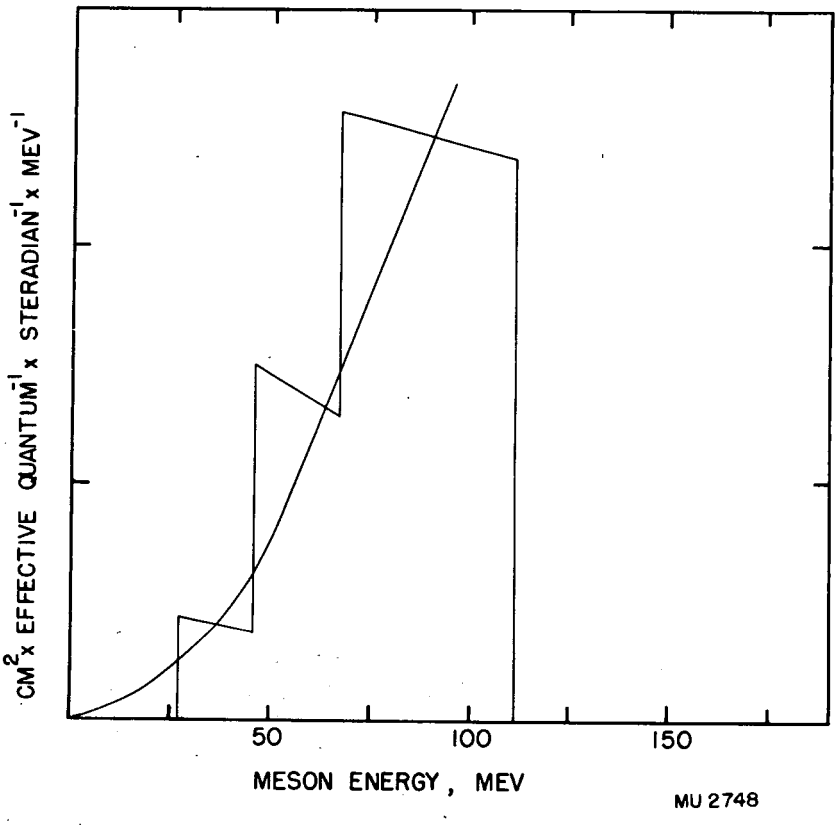
CM^2 x EFFECTIVE QUANTUM^{-1} x STERADIAN^{-1} x MEV^{-1}
50
100
150
MESON ENERGY, MEV
MU 2748

Fig. 13